Giant hysteretic magnetoresistance accompanying the Mott transition and spin-glass state in the organic metal κ-(BEDT-TTF)$_2$Hg(SCN)$_2$Br

P. D. Grigoriev [1,2,3] S. I. Pesotskii [4] R. B. Lyubovskii,[4] S. A. Torunova [4] D. S. Lyubshin [1] and V. N. Zverev [5]

[1] *L. D. Landau Institute for Theoretical Physics, 142432 Chernogolovka, Russia*

[2] *National University of Science and Technology "MISIS", 119049 Moscow, Russia*

[3] *National Research University Higher School of Economics, Moscow 101000, Russia*

[4] *FRC of Problems of Chemical Physics and Medicinal Chemistry RAS, Chernogolovka, Moscow Region, 142432, Russia*

[5] *Institute of Solid State Physics RAS, Chernogolovka, Moscow Region 142432, Russia*

(Received 22 July 2025; revised 19 February 2026; accepted 24 February 2026; published 23 March 2026)

The giant magnetoresistance with a huge hysteresis is observed in the organic metal κ-(BEDT-TTF)$_2$Hg(SCN)$_2$Br at low temperature in a pressure interval around 3 kbar of a width ~1 kbar. The hysteretic magnetoresistance is isotropic with respect to the direction of magnetic field, which excludes the orbital effect of magnetic field as its origin. The observed temperature and magnetic-field dependence of this hysteresis and of its relaxation time indicates the strong influence of the spin-glass state on magnetoresistance. Although a quantitative theory of this effect, originating from strong electronic correlations, requires complex numerical calculations, we suggest its explanation and a simple model which qualitatively describes the observed magnetoresistance behavior and shows a strong charge-spin entanglement. The proposed effect suggests another class of extreme magnetoresistance mechanisms.

DOI: 10.1103/j565-gnd6

I. INTRODUCTION

The giant magnetoresistance (GMR) is a subject of huge research activity because of interesting physics and promising applications for magnetic field sensors (e.g., see Refs. [1,2] for reviews). There are many possible mechanisms of GMR. The magnetic multilayer structures, where magnetization is controlled by an external field, give GMR which has already been applied in technology [1,2]. Another GMR mechanism associated with a ferromagnetic-to-paramagnetic phase transition, known as colossal magnetoresistance (CMR) [3], has already been actively investigated for 30 years [3–5]. The extremely large magnetoresistance (XMR) includes several different mechanisms [6], most pronounced at low temperatures. Usually, all these mechanisms can be understood in the one-electron approximation, i.e., when the electron-electron (e-e) interaction can be neglected.

Another important area of the condensed matter physics deals with strong electronic correlations. The high-T_c superconductivity, charge- and spin-density waves, Mott metal-insulator transitions (MITs) and many other interesting and promising phenomena cannot be properly described without the e-e interaction. Usually, the GMR and strongly correlated electronic systems are not directly coupled. Below we propose and investigate the system where GMR originates from strong electronic correlations. We report both the detailed experimental analysis and a theoretical description of GMR originating from electronic correlations. In addition to the usual shift of Mott metal-insulator transition by a magnetic field [7–11], the compound κ-(BEDT-TTF)$_2$Hg(SCN)$_2$Br studied here also hosts a spin-glass state coupled to electronic charge ordering [12,13].

The organic metal κ-(BEDT-TTF)$_2$Hg(SCN)$_2$Br belongs to the well-known family of quasi-two-dimensional conductors, which are single crystal samples of cation—radical salts in which flat organic molecules of BEDT-TTF form cationic layers alternating with inorganic anionic ones. When the salt is formed, an electron from every second BEDT-TTF molecule goes to the anion. The remaining electrons, moving between BEDT-TTF molecules, form a three-quarters-filled hole metal band inside the layers, the conductivity of which is several orders of magnitude higher than the conductivity between the layers [14]. In samples with packaging of BEDT-TTF molecules in the κ-type layer, such molecules form dimers that create a geometrically frustrated flat triangular lattice, which leads to the splitting of the conduction band into a completely filled and half-filled one [15]. This circumstance, as well as the narrow conduction band, $W \sim 0.2$ eV [16], create the necessary conditions $U/W > 1$ for the transition of the metal κ-(BEDT-TTF)$_2$Hg(SCN)$_2$Br to the Mott-insulator state, where U is the Coulomb repulsion energy on one dimmer. Indeed, in this metal, during cooling, a MIT was detected in the temperature dependence of the resistance at $T_{\mathrm{MI}} \sim 90$ K [17], and the state below the transition temperature was interpreted as a state similar to a Mott insulator. The low-temperature state was studied by various methods at ambient pressure [12,17–19]. Evidence was found of a spin-glass state in the spin system at temperatures below 20 K [12] and a dipole liquid state in the charge system [12,13]. Both of these states are a consequence of the original lattice frustration. At $T \sim 90$ K, the metal κ-(BEDT-TTF)$_2$Hg(SCN)$_2$Br also undergoes a structural phase transition [16] from a monoclinic syngony above 90 K to a triclinic one below 90 K. This transition is accompanied by a pronounced hysteresis

 ©2026 American Physical Society

in the temperature dependence of the resistance. Theoretical calculations of the band structure showed [16] that the triclinic lattice corresponds to an alternative but also metallic electronic structure, unstable to the Mott-insulator transition. The application of external pressure reduces the distance between the dimers and increases the width of the conduction band W, suppressing the Mott transition.

At a pressure of $p = 5$ kbar, Shubnikov–de Haas oscillations with a frequency of $F \approx 240$ T were detected in the quantizing magnetic field in a good agreement with the theoretical calculations of the band structure for the triclinic lattice. A further increase in pressure leads to an increase in the magnitude of magnetoresistance and in the amplitude of quantum oscillations with the same frequency. As a result, it is assumed that localized and delocalized electrons coexist in the entire pressure range $p = (1 - 8)$ kbar. Below we show data confirming the spin-glass state in κ-(BEDT-TTF)$_2$Hg(SCN)$_2$Br at low temperatures and analyze the effect of such a state on the magnetoresistance behavior near the MIT. A strong magnetoresistance at the Mott MIT was investigated before [7–11], but we argue that our case differs from the standard theory [8–10] because of spin frustrations on a triangular lattice and of the strong entanglement between spin state and charge transport.

In Sec. II, we provide our experimental data on a strong magnetoresistance with a huge hysteresis at pressure around 3 kbar of the Mott transition in a magnetic field $B < 16$T. These data show the dependence of this hysteretic magnetoresistance on temperature, pressure, and magnetic field. At first glance, the observed strong influence of the rather weak Zeeman splitting $\lesssim$10 K on a Mott MIT with a much larger energy scale $\sim T_{\rm MI} = 90$ K is very surprising. In Sec. III, we explain this interesting effect and illustrate it on a toy model. In Sec. IV, we discuss our results and theoretical model and indicate some qualitative differences between the proposed and previously known magnetoresistance mechanisms.

II. EXPERIMENTAL RESULTS

Sample resistance was measured using a standard four-probe method by a lock-in detector on single crystals with characteristic sizes of $1.0 \times 1.0 \times 0.1$ mm^3. Two contacts were prepared to each of two opposite sample surfaces with conducting graphite paste. A measuring current with a frequency of 20 Hz, the value of which did not exceed 1 μA, was directed perpendicular to the conducting layers of the crystal, so we have measured the out-of-plane sample resistance. The samples were mounted in a high-pressure chamber filled with silicon oil, which ensured operation under quasihydrostatic conditions at low temperatures. The pressure was measured by the manganin probe; in all figures, we show the value of the pressure corresponding to the low-temperature region. The measurements were carried out in the variable temperature insert that allowed working in the temperature range from the room temperature down to 1.3 K. A magnetic field of up to 7 T was created by a superconducting solenoid and directed either perpendicular or along the conductive layers of the crystal.

As we previously established [16], in the samples of κ-(BEDT-TTF)$_2$Hg(SCN)$_2$Br at $T \approx 90$ K, a structural phase transformation accompanied by Mott MIT takes place.

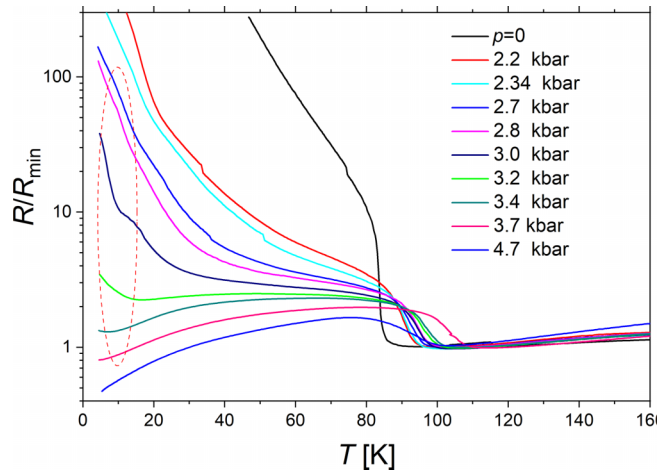


FIG. 1. Temperature dependencies of the reduced interlayer resistance $R/R_{\rm min}$ of the sample κ-(BEDT-TTF)$_2$Hg(SCN)$_2$Br at different pressures. $R_{\rm min}$: the resistance value at minimum on the $R(T)$ dependence in the region of structural phase transition.

Figure 1 shows the temperature dependencies of the interlayer resistance in κ-(BEDT-TTF)$_2$Hg(SCN)$_2$Br at various pressure values. When the temperature goes down, the sample resistance decreases, but at $T \approx 90$ K the resistance sharply increases due to the MIT. External pressure reduces the sample resistance and suppresses the MIT without changing the crystal structure. At ambient pressure and room temperature, this resistance is $R \approx$ 130 ohms. At the pressure corresponding to the lowest curve in Fig. 1, the resistance drops down to 64 ohm. All curves shown in Fig. 1 were recorded at a decrease of temperature. Therefore, the hysteresis associated with the structural transition, i.e., shift of transition temperature by about 5 K during the up and down temperature sweeps, is not represented here. In the present work, in contrast to Ref. [16] where the magnetotransport was studied in a metallic state, we focus on the study of low-temperature magnetoresistance in the MIT pressure region 2.5 kbar $< p <$ 4 kbar. This area is highlighted in Fig. 1 by a red dotted oval.

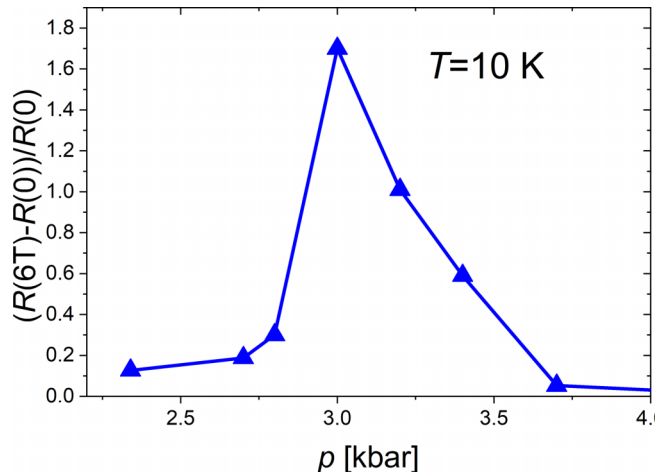


FIG. 2. Sample magnetoresistance $(R(6T) - R(0))/R(0)$ at $T = 10$ K as function of pressure.

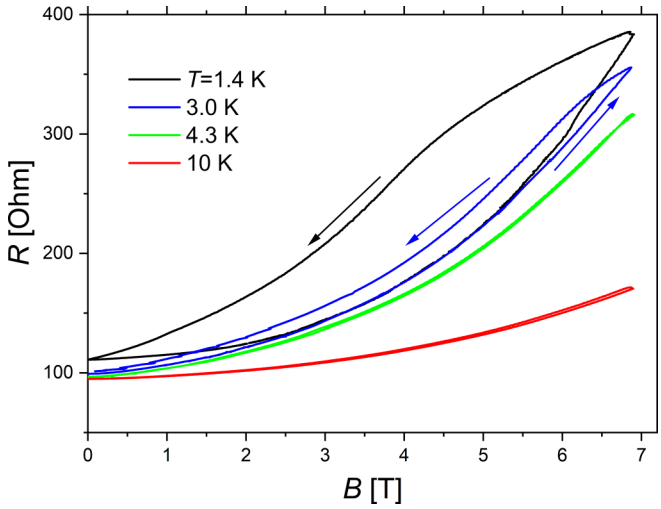


FIG. 3. $R(B)$ dependence at various temperatures and pressure $p = 3.4$ kbar.

Figure 2 shows the pressure dependence of magnetoresistance $\Delta R/R = [R(6T) - R(0)]/R(0)$ at a relatively high fixed temperature $T = 10$ K. It illustrates an abnormal increase in magnetoresistance in the MIT region, exceeding 150% at a pressure of about 3 kbar. Note that at pressures both above and below the transition region, $\Delta R/R$ does not exceed 10% at the same temperature.

The most interesting $R(B)$ results were obtained in the low-temperature region $T < 10$ K. Figure 3 shows these results at pressure $p = 3.4$ kbar. As one can see from this figure, the magnetoresistance increases dramatically with the decrease of temperature, and a strong hysteresis occurs on the $R(B)$ dependencies. Similar curves were obtained at pressures from 2.8 to 3.7 kbar, which is illustrated in Fig. 4, where the $R(B)$ dependencies are shown for various pressures at $T = 1.4$ K. The hysteresis is present on all curves in Fig. 4, being almost invisible on the lowest one for p=3.7 kbar in this scale, because the maximum loop width on this curve is approximately 1%, while at $p = 3.4$ kbar the loop width exceeds 50%.

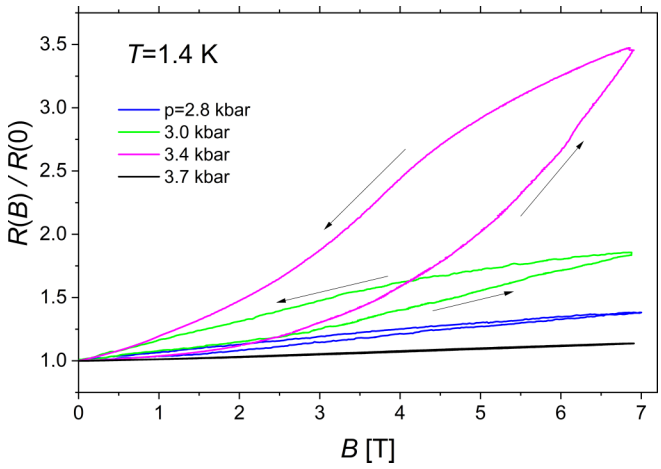


FIG. 4. $R(B)$ dependencies at various pressures. T=1.4 K.

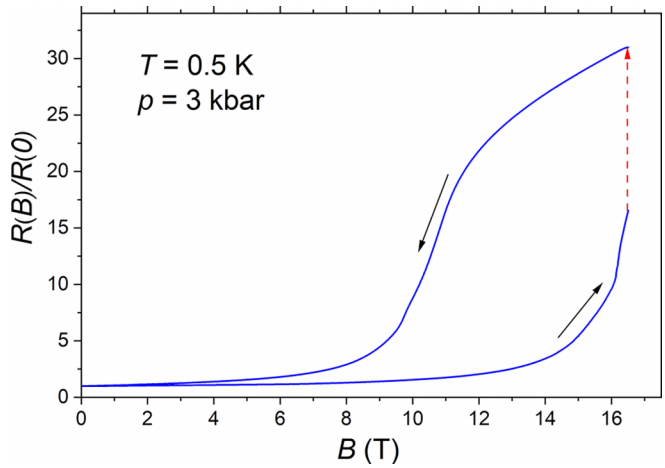


FIG. 5. $R(B)$ dependence at $p = 3$ kbar and $T = 0.5$ K.

It is noteworthy that in Figs. 3 and 4, the presented $R(B)$ curves do not depend on the magnetic field sweep rate below 0.4 T/min., i.e., with a fixed field B at any point on the curve $R(B)$, the sample resistance practically does not change over time. When the field sweep was stopped, a slight increase in the sample resistance was observed, not exceeding a few percent for several tens of seconds. A different behavior appears at higher fields and lower temperatures. Under these conditions, the effects of long-term resistance relaxation were observed: the sample resistance increased significantly at a fixed magnetic field with a characteristic time of about an hour. Figure 5 demonstrates this effect at a pressure 3 kbar in a field of 16.5 T and a temperature of 0.5 K. The resistance growth at a fixed magnetic field is shown by the red vertical arrow. The observation of such a long relaxation time was the main reason for conducting our experiments at higher temperatures and lower magnetic fields.

In control experiments, we performed the magnetoresistance measurements in a geometry when the magnetic field was directed along the conducting layers of the sample. It turned out that in this case hysteresis is also observed and even more pronounced compared to the $B||c$ case. Figure 6 shows the $R(B)$ dependence at a pressure of 2.9 kbar in the case when the field is parallel to conductive layers. The comparison of these data with those shown in Fig. 4 shows that the observed effects in this geometry are much more pronounced: At $T = 1.4$ K the hysteresis loop is significantly wider, and the magnetoresistance is several times greater even compared to the curve at p=3 kbar in Fig. 4.

Since we recorded the influence of the magnetic field on the sample resistance depending on the prehistory, we compared the $R(T)$ dependencies both for zero field cooling (ZFC) and for field cooling (FC) regimes. It turned out that in the ZFC mode, the sample resistance at the final low temperature is several times lower than that in the case of the FC mode. In addition, we determined the value of magnetic field required to transfer the sample to a state corresponding to FC regime. The results of these measurements are shown in Fig. 7 for the case where the field was directed along the planes of conducting layers. In the case where the field was directed perpendicular to the layers, we obtained a similar result.

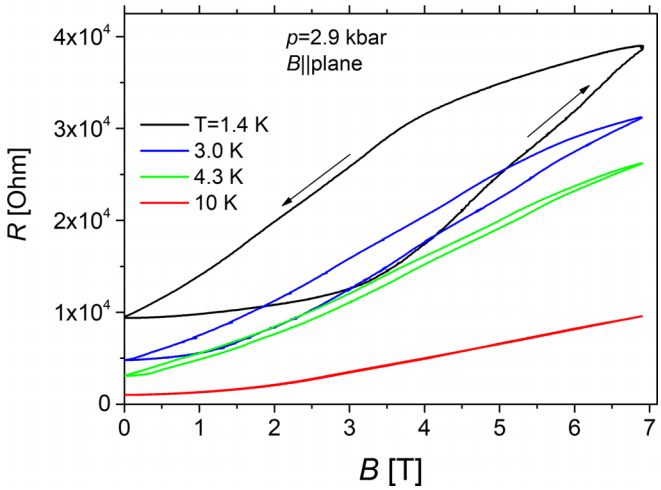


FIG. 6. $R(B)$ dependencies at various temperatures and fixed pressure p=2.9 kbar in the geometry when magnetic field lies in the plane of conducting layers.

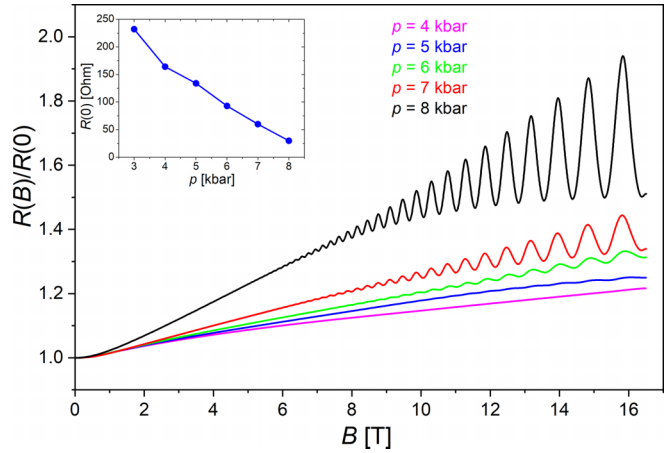


FIG. 8. Magnetic quantum oscillations at T=0.5 K and various pressures. The pressure dependence of the sample resistance at $B = 0$ is shown in the inset.

The resistance values obtained in ZFC and FC modes are indicated in Fig. 7 by arrows. Starting from the ZFC state, we successively cycled the magnetic field, increasing it to the values 1, 2,... 7 T, each time returning to the point B=0. As can be seen from the figure, with a successive increase in the field to 1, 2, and 3 T, the hysteresis loops did not close, and the final resistance was higher than the starting one. However, with an increase in the field to 4 T, the sample resistance returns at B=0 directly to the value corresponding to the FC mode, while further cycling the field to larger values already leads to a closed hysteresis loop, i.e., to the FC state.

As we have argued in Ref. [16] and pointed out in the Introduction, free and localized electrons may coexist, and the fraction of free electrons increases with pressure. This statement is illustrated by Fig. 8, which demonstrates the low-temperature magnetoresistance in the metallic state at magnetic field perpendicular to conducting layers. One can see that the higher the pressure, the smaller the sample resistance (see the inset to Fig. 8). Moreover, the relative amplitude of the Shubnikov–de Haas oscillations increases dramatically with increasing pressure, while the oscillation frequency does not change. These observations mean that we really deal with the coexistence of insulating and conducting phases, and the fraction of conductive phase increases with pressure.

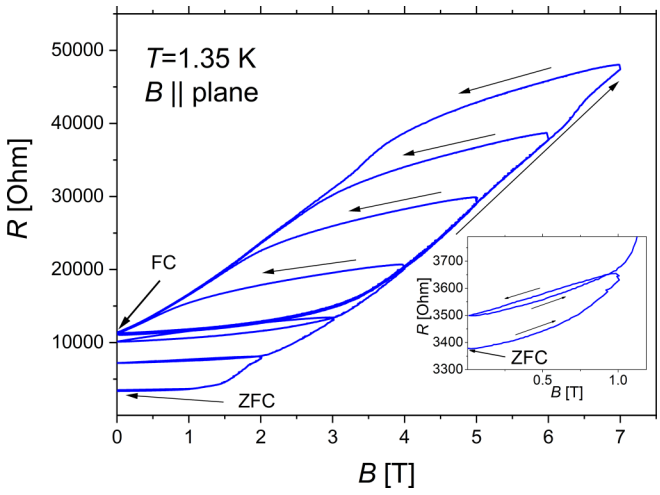


FIG. 7. $R(B)$ dependencies for cyclic changes of magnetic field from zero to values 1, 2,... 7 T at T = 1.35 K. Starting value corresponds to the resistance obtained in field-free cooling mode (ZFC). The inset shows the first cycle on an enlarged scale, which is practically invisible in the main figure.

III. THEORETICAL DESCRIPTION

Let us summarize the main experimental observations and their current understanding. The interdimer electron transfer integrals t, t', which in metals determine the conducting bandwidth, are rather small in κ-(BEDT-TTF)$_2$Hg(SCN)$_2$Br and comparable to the Coulomb energy. This leads to the MIT at ambient pressure at $T_{\rm MI} \approx 90$ K [17]. Note that at the same temperature, the structural phase transition also happens [16]. This combined structural and electronic phase transition is of the first order, as experimentally confirmed by the sharp peak of specific heat and by both resistivity [16] and susceptibility hysteresis at $T \approx T_{\rm MI}$ (see Fig. 5 in Ref. [12]). Hence, the heterogeneous state with both metallic and insulating phases may appear near the MIT. An external pressure p reduces the interdimer distance, increasing the interdimer transfer integrals t, t' and favoring the metallic phase. Hence, the external pressure increases the volume fraction of the metallic phase. At $p > p_c \approx 3$ kbar, the metallic conductivity is observed till very low temperatures, corresponding to the quantum phase transition.

We observe a giant magnetoresistance in κ-(BEDT-TTF)$_2$Hg(SCN)$_2$Br at the Mott transition, see Fig. 2, which becomes much stronger at low temperature (see Figs. 3–8). This effect is not new in organic metals and was previously investigated in κ-(BEDT-TTF)$_2$Cu[N(CN)$_2$]Cl [11]. The common theoretical description of this magnetoresistance is based on the following. The magnetic susceptibility χ near the Mott transition diverges in the Gutzwiller's approximation [7] or strongly increases according to the numerical

calculations based on the Hubbard model at half filling in the controlled limit of infinite spatial dimensionality [8,9], which is actually a dynamic mean field theory (DMFT) method [10]. Hence, the external magnetic field $\boldsymbol{B}$ may considerably influence the Mott phase transition and shift the transition line, thereby giving rise to magnetic-field-induced Mott transition, or magnetoresistance. When $\boldsymbol{B}$ shifts the system toward the Mott-insulating phase, it increases the electric resistivity, leading to positive magnetoresistance. This explanation is adopted, e.g., in Ref. [11].

However, our case has several important differences from the usual case, described by the standard theory [8–10]. First, we observe a huge hysteresis in κ-(BEDT-TTF)$_2$Hg(SCN)$_2$Br, and it happens at temperatures much below the Mott MIT but close to the spin-glass transition temperature. As seen in Fig. 5, the magnetoresistance value $(R(16.5\ \mathrm{T})\text{-}R(0))/R(0)$ at 0.5 K is about 30 (i.e., 3000% !), but already at $T \sim 10$ K, which is still much lower than the Mott-insulator transition temperature $T_{\mathrm{MI}} \approx 90$ K, magnetoresistance is by an order of magnitude smaller (see Fig. 3). Note that the hysteresis at $T_{\mathrm{MI}} = 90$ K, associated with the first-order Mott phase transition as described by standard theory [8–10], is also present (see Fig. 5(b) of Ref. [12] and Fig. 2(b) of our previous paper [16]), but this hysteresis has a narrow temperature range around $T_{\mathrm{MI}} = 90$ K and closes at $T < 87.5$ K, indicating that it is completely different from the hysteresis at $T < 10$ K studied in the present paper.

There are several important differences between the hysteretic magnetoresistance observed in our compound κ-(BEDT-TTF)$_2$Hg(SCN)$_2$Br and in κ-(BEDT-TTF)$_2$Cu[N(CN)$_2$]Cl, where there is no spin-glass state and the standard theory [8–10] is usually applied [11]. While in κ-(BEDT-TTF)$_2$Hg(SCN)$_2$Br the temperatures of metal-insulator transition and of magnetoresistance hysteresis differ by an order of magnitude, in κ-(BEDT-TTF)$_2$Cu[N(CN)$_2$]Cl they are rather close. The Mott metal-insulator transition in κ-(BEDT-TTF)$_2$Cu[N(CN)$_2$]Cl happens at $T_c \sim 30$ K, while the strong magnetoresistance hysteresis is observed already at $T = 22.2$ K (see Fig. 2(a) in Ref. [11]). The difference between the shapes of magnetoresistance hysteresis in these two compounds is also notable. In κ-(BEDT-TTF)$_2$Cu[N(CN)$_2$]Cl the magnetic field simply shifts the sharp jump of magnetoresistance (see Fig. 2 in Ref. [11]), while in κ-(BEDT-TTF)$_2$Hg(SCN)$_2$Br our experimental data (see Figs. 3–7) demonstrate much smoother curves, typical of glass behavior rather than sharp transitions.

Both the magnetoresistance and the width of hysteresis loop increase with the field and with the drop of temperature. The observed dependence of magnetoresistance on prehistory (see Fig. 7) is obviously related to the influence of frustrated spin systems and of the corresponding spin-glass state on the measured resistance. From Fig. 7, one sees that the hysteresis loops close if the field $B \geqslant 4$ T, when the Zeeman energy $E_Z \sim 5$ K is much greater than $T = 1.35$ K. The characteristic temperature when the strong hysteresis appears has a close magnitude $T_{\mathrm{hyst}} \sim 5$ K (see Fig. 6). This temperature $T_{\mathrm{hyst}} \sim E_Z$ is much lower than the Mott-insulator transition temperature $T_{\mathrm{MI}} \approx 90$ K, indicating that the observed hysteresis is not determined by the Mott-insulator transition only, as implied in the standard theory [8–10]. The hysteresis energy scale $T_{\mathrm{hyst}} \sim E_Z \sim 5$ K is very close to the temperature $T_m \approx 5$ K of excess peak in heat capacity, attributed to the glass behavior [12]. On the other hand, the entropy contained in the excess peak $S = 13.7$ J/mol K is significantly larger than the pure magnetic entropy of the spin-1/2 system ($S = R \ln 2$), indicating that the glassy state largely involves the charge degree of freedom, resulting in a charge-spin entanglement [12]. Our model below qualitatively describes the physics of this entanglement.

Second, the observed very slow relaxation of magnetoresistance (see Fig. 5) also unambiguously indicates the strong influence of the spin-glass state, having this slow dynamics (see Supplemental Material [20]), on magnetoresistance. The energies of states with opposite spins in the field differ by ΔE_Z, so the change in the configuration of the spin system occurs over a time that depends on the field and temperature: it increases with decreasing T and increasing B.

Third, even with the enhanced susceptibility near the Mott phase transition, the simple thermodynamic effect of magnetic field is, probably, not sufficient to strongly shift the balance between Mott-insulating and metallic phases because of a large difference of energy scales. The magnetic field $B \leqslant 7$ T even at saturation of magnetization introduces the energy scale of Zeeman energy $E_Z \sim \mu_B B < 10$ K per electron, while the Mott MIT temperature is 90 K, and the corresponding activation energy $E_g \sim 20$ meV ≈ 230 K [17] is even higher. The formation of the energy gap E_g at the Fermi level with density of electron states ν_F gives the energy gain $\sim E_g^2 \nu_F/2$ of the Mott-insulating phase, which considerably exceeds the magnetic energy gain $\chi B^2/2$. This comparison is easier to perform per one electron. The energy gain from the formation of a Mott energy gap at the Fermi level is $\Delta E_{\mathrm{MI}} \sim E_g^2/2E_F$ per one electron [21], where E_F is the Fermi energy in the metallic phase. In κ-(BEDT-TTF)$_2$Hg(SCN)$_2$Br, the band structure calculations give [16] $W \approx 0.2$ eV, and the corresponding Fermi energy at half filling is $E_F \sim 0.1$ eV. Substituting the numbers, we get the energy gain $\Delta E_{\mathrm{MI}} \sim E_g^2/2E_F \approx 0.002$ eV$\sim$25 K per electron in the conducting band, which considerably exceeds the upper limit of magnetic energy gain E_Z from these electrons. Indeed, even at complete spin polarization of conducting band, the magnetic energy gain is $E_{\mathrm{mag}} < E_Z \approx \mu_B B < 8$ K per one electron at field $B \leqslant 7$ T. Due to the antiferromagnetic coupling on a triangular lattice, a considerable fraction of spins is not aligned along the magnetic field, which additionally reduces E_{mag} by a factor $\sim$3. In a metallic state, the magnetic energy gain from conducting electrons E_{mag} is additionally reduced by a factor $\sim E_Z/E_F < 0.01$. Hence, even with the enhanced susceptibility near the Mott phase transition, the simple thermodynamic effect of magnetic field is not sufficient to strongly shift the Mott transition line. Below we argue that the effect of magnetic field in κ-(BEDT-TTF)$_2$Hg(SCN)$_2$Br is not reduced to simple thermodynamics because the spin alignment directly affects the electron transport.

Although the magnetic field evidently shifts the Mott transition line according to the standard DMFT theory [7–10], we believe that this theory is not sufficient to explain all observed features of the Mott transition in κ-(BEDT-TTF)$_2$Hg(SCN)$_2$Br. The spin frustrations on a triangular lattice must be included into the model as they play an essential

role in physical processes. This is especially reflected in slow relaxation and giant hysteresis, common for a spin-glass state. The Hubbard model on a triangular lattice has received considerable theoretical attention [22–26], but the effect of external magnetic field on this system was not sufficiently investigated. There may be additional difficulties of applying the standard DMFT methods with a local self-energy part to the spin-glass system where the nonlocal effects are essential. Below we do not perform novel DMFT calculations for the half-filled Hubbard model on the triangular lattice in a magnetic field, but propose a simple qualitative model which, in our opinion, captures the essential physics of the observed giant magnetoresistance with a huge hysteresis and slow relaxation at low temperature. It also helps us understand the physical mechanisms behind the complicated *ab initio* calculations.

A. Qualitative description

To present our qualitative idea behind the proposed colossal magnetoresistance mechanism and its hysteretic behavior, we first emphasize several features of κ-(BEDT-TTF)$_2$Hg(SCN)$_2$Br. The conducting layers of the dimerized BEDT-TTF molecules host one electron per dimer. The dimer size is $d \sim 1$ nm, and the dimensional quantization on this small size gives a large energy splitting $\Delta E_d \sim \hbar^2/(md^2) \sim 0.1\ \text{eV} \gg T \sim 2\ \text{K}$. The electrons mainly occupy only the lowest energy level on each dimer. The spins of these electrons couple antiferromagnetically with similar electrons on neighboring dimers [12]. The opposite spin orientations of neighboring electrons allow interdimer jumps which delocalize the electron wave functions, thus lowering the electron kinetic energy. It also enhances the electron conductivity and favors the metallic behavior. For ferromagnetic spin orientation on adjacent dimers, the interdimer jumps is forbidden by Pauli exclusion principle. We call such a ferromagnetically ordered spin configuration of electron pairs on adjacent dimers *current-locking*.

The triangular lattice of BEDT-TTF dimers leads to geometrical magnetic frustrations and spin-glass behavior instead of long-range AFM order [12]. The observed excess peak in the specific heat at $T = T_m \approx 5\,\text{K}$ and the strong increase of magnetic susceptibility at $T < 30\,\text{K}$ (see Fig. 5 in Ref. [12]) can be attributed to magnetic frustrations and even result to weak ferromagnetism in the form of isolated small ferromagnetic puddles [12]. The magnetic frustrations are also consistent with the observed inhomogeneous NMR line broadening at $T < 40\,\text{K}$ and with the strong increase of the nuclear spin relaxation rates $1/T_1$ and $1/T_2$ at $T < 20\,\text{K}$ [19]. Because of the frustrations, some neighboring electron spins have the same projection, which forbids interdimer hopping between them and reduces conductivity. The typical energy difference between two opposite spin projections is also reduced by the frustrations and is of the order of the temperature of specific-heat maximum $T_m \approx 5$ K.

A moderate magnetic field $B \gtrsim 1$T, resulting in Zeeman energy splitting $\Delta E_Z \gtrsim 2\,\text{K} \sim T_m$, may strongly change the spin-glass state by aligning a considerable part of electrons on dimers along the magnetic field. This strong response of spin glass in κ-(BEDT-TTF)$_2$Hg(SCN)$_2$Br is supported by the strong enhancement at $T < 20\,\text{K}$ and even the divergence of magnetic susceptibility at $T \to 0$, as shown in Fig. 4(b) of Ref. [12]. This increases the number of current-locking ferromagnetically ordered adjacent electron spins in a magnetic field. Hence, it shifts the Mott MIT toward the insulating phase, which results to a strong magnetoresistance in the vicinity of MIT.

All the above referred to the spin system in the dielectric regions of the sample. However, we emphasize that we measure the resistance of the sample, using it as a sensor of the spin system's state, i.e., the resistance clearly reflects the state of the spin glass. Therefore, the observed effects (giant magnetic resistance, hysteresis, and temporal relaxation) in combination with clear magnetic quantum oscillations (MQOs) can be explained by the contribution of both metallic and Mott-insulating regions to the measured resistance when the current passes sequentially through these regions.

The magnetoresistance hysteresis appears due to the hysteretic behavior of spin-glass configuration with magnetic field variations. For each value of external magnetic field, the spin-glass system has a new set of local energy minima and of the corresponding spin configurations. The system chooses a local energy minimum, which is far from the global minimum. The relaxation of this spin-glass system is rather slow. In our experiment at $B = 16.5\,\text{T}$ and $T = 0.5\,\text{K}$ (see Fig. 5), when $\Delta E_Z \gg T$, the typical relaxation time of the resistivity was about one hour, but in a weaker magnetic field and higher temperature the relaxation time is much smaller. This strong magnetic-field dependence of relaxation time indicates that the spin glass is involved. Hence, a typical glassy properties of the relaxation time observed in κ-(BEDT-TTF)$_2$X family by fluctuation spectroscopy studies [27] is related not only to charge but also to spin dynamics. When the magnetic field increases, the system chooses a local minimum which is closer to its zero-field configuration, where the number of AFM spin bonds is maximal. This favors the metallic phase. When the magnetic field decreases, the system chooses a local minimum which is closer to its high-field almost spin-polarized configuration, where the number of current-locking ferromagnetic spin bonds is maximal, favoring the insulating phase. Hence, at the same conditions, the resistivity in a raising magnetic field is smaller than in a decreasing field.

The above idea describes qualitatively both the giant magnetoresistance and its hysteresis at the Mott-Hubbard phase transition, as we observed in κ-(BEDT-TTF)$_2$Hg(SCN)$_2$Br at pressure $\sim$3 kbar. A quantitative theory of this unusual magnetoresistance behavior, originating from strong electronic correlations, requires at least complex and lengthy numerical calculations, e.g., using DMFT (see, e.g., Refs. [28,29] for reviews). This description is additionally complicated by the presence of magnetic field, spin frustrations, nonlocal spin-glass behavior, and subsequent conductivity calculations. While DMFT often gives a reasonable band structure at the Mott-Hubbard phase transition on a large energy scale $\gtrsim$0.1 eV [28,29], calculating electron transport properties using the derived electronic structure, especially in a magnetic field, requires precise details that are not typically captured by DMFT. The available DMFT calculations of the Hubbard model at half filling in a magnetic field [8–10] do not take into account the spin frustrations and glassy behavior on a

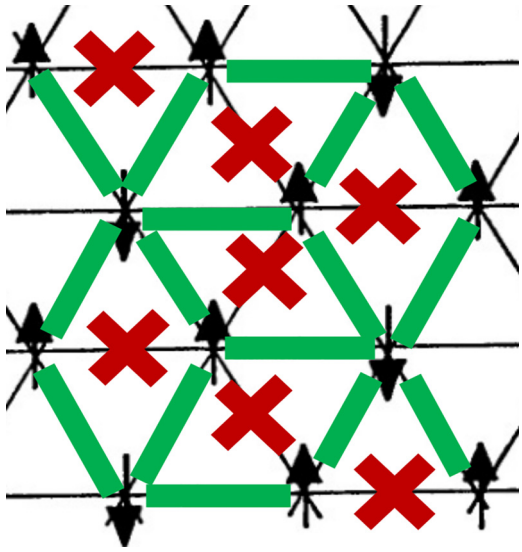


FIG. 9. Schematic illustration of the classical toy model of a triangular lattice with one electron per site on the Fermi level. The electrons may hop to the nearest sites, but the probability of this hopping depends very much on the mutual spin orientation of the electrons on these two nodes. Therefore, the nearest sites of this triangular lattice are connected by the resistances of two values R_1 (green thick lines when the electron spins are antiparallel) and $R_2 \gg R_1$ (red crosses), corresponding to the same spin orientation on these nearest sites.

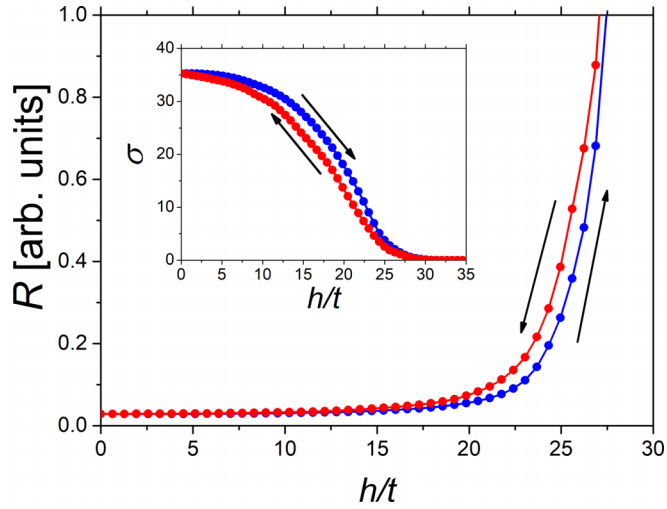


FIG. 10. Calculated giant magnetoresistance $R(B)$ in our toy model for increasing (blue symbols) and decreasing (red symbols) magnetic field. The magnetic field $h/T \propto B$ is normalized as the ratio of Zeeman energy $h = \Delta E_Z/2$ to temperature T. Inset shows the conductivity $\sigma(B) = R^{-1}$ for the same parameters, where the hysteresis is clearer seen.

triangular lattice. Therefore, to illustrate that the observed giant hysteretic magnetoresistance indeed originates from the above qualitative arguments, and that the spin frustrations and spin-glass behavior strongly affect the magnetoresistance, we consider a simple classical toy model, as described below.

B. Toy model

Consider a 2D triangular lattice of spins up or down (see Fig. 9), which models the conducting electrons on the molecular dimers in κ-(BEDT-TTF)$_2$Hg(SCN)$_2$Br in one conducting layer. Most of the time, each node of this triangular lattice is occupied by one conducting electron because two electrons on one dimer cost an extra Coulomb energy. Nevertheless, the electrons may hop from one node to a nearest node, but the probability of this hopping depends very much on the mutual spin orientation of the electrons on these two nodes: the hopping to the same orbital quantum state is prohibited by the Pauli exclusion principle if two electrons have the same spin projection and is allowed for different spin orientations. Therefore, the nearest nodes of a triangular lattice in our toy model are connected by the resistances of two values R_1 (green thick lines in Fig. 9) and R_2 (red crosses in Fig. 9). The largest resistance $R_2 \gg R_1$ connects the nearest neighbors with the same spin projection of conducting electrons, when the intersite hopping is almost prohibited. Hence, the Ising system of spins on a triangular lattice, easily controlled by external magnetic field, affects strongly the electron conductivity and produces magnetoresistance.

The phase diagram of a classical 2D Ising model on a triangular lattice is well-known [30], but we are interested in the resistance of the lattice affected by its spin configuration and driven by the external magnetic field. Somewhat similar resistive Ising model was studied recently [31], where the random-graph nanowire network tunnel junctions also take binary conductance values depending on mutual magnetic orientation. However, the different geometry in Ref. [31] gives a completely different phase diagram and resistance behavior, not applicable to our system. The memristive Ising circuits [32] also have no direct relevance to our system but may give its further prospects.

In Fig. 10, we show the results of our numerical calculation of resistivity and conductivity in the proposed toy model as a function of increasing (blue symbols) and decreasing (red symbols) magnetic field. One clearly sees both a giant magnetoresistance and a considerable hysteresis near the metal-insulator transition, as observed in our experiment. In the Supplemental Material [20], we give the details of this calculation, including the dependence of the results obtained on various parameters: temperature T, exchange magnetic coupling J of conducting electrons on the closest dimers, the resistance ratio R_2/R_1, the speed of the variation of magnetic field, and on the disorder in exchange coupling.

IV. DISCUSSION

The proposed classical toy model does not pretend to explain our results quantitatively, but it demonstrates the main idea of our interpretation of the observed phenomena. In particular, it describes well the giant magnetoresistance, as shown in Fig. 10. In addition, it gives a hysteresis, which is better seen on the conductivity plot in the inset in Fig. 10. It also gives the observed glassy properties of relaxation times (see Supplemental Material [20], Figs. 13–17). However, to obtain a hysteresis in our model one has to introduce a disorder to the frustrated spin system, e.g., in the exchange coupling constants. This observation, that the disorder is necessary for hysteresis in addition to a geometrical frustration, is not the

peculiarity of our model and agrees with the known general theory of frustrated spin systems [33,34]. There are several reasons for the disorder in organic conductors. First, the orientational disorder in conformation of ethylene groups (eclipsed or staggered) of terminal ethylene groups of ET molecules may exist [35–38]. Second, the disorder may appear due to the charge disproportionation on ET molecules [39]. Third, the disorder may also originate from electron dynamics. Indeed, the exchange coupling strongly depends on the overlap of electron wave functions. Due to the Coulomb interaction and strong electron correlations, the electron wave functions on each dimer depend on other electrons and on their spins, which may (slowly in comparison to fast electron dynamics) change with time due to spin relaxation, especially when the magnetic field varies. Therefore, the proposed toy model of classical resistances does not give a quantitative agreement of the hysteresis width because it does not solve the complicated problem of strong electronic correlations properly. In particular, we consider only the effect of external magnetic field on the frustrated electron spins, which affects electronic transport. However, the spin-dependent interaction between conducting electrons does not include the back influence of electron transport and dynamics on their spin configuration.

The proposed toy model is 2D, while in experiment we have a layered 3D material. One can generalize the numerical calculations to a 3D case but the result will be qualitatively the same, while it requires a much larger calculation time. Indeed, similar to the intralayer 2D transport, the interlayer hopping of conducting electrons between the adjacent dimers will be hindered or nearly prohibited by the Pauli principle if the electron spins are the same and allowed for opposite spins. The external magnetic field due to the Zeeman energy gain orients more electron spins along the magnetic field, thus increasing the number of forbidden hopping directions and the total resistivity both along and across the conducting layers. In addition, there is a general rule known from various MIT driven by disorder [40] that if electrons in a metal become more localized in some directions, this also reduce conductivity and often produce localization along all directions.

In the current classification of different GMR mechanisms, the proposed GMR mechanism is closer to XMR [6] because it originates neither from magnetic layers of different magnetization, as in usual GMR [1,2], nor from a ferromagnetic-to-paramagnetic phase transition inherent to CMR [3–5]. In both these standard mechanisms, the crucial role is played by the electron scattering on the macroscopic boundary between two areas of different magnetization, either between two layers of different material and magnetization (GMR) or between ferromagnetic and paramagnetic phases (CMR), which also have different magnetizations. In our mechanism, there is no scattering by any macroscopic boundary, necessary for usual GMR and CMR mechanisms.

Contrary to most GMR, our mechanism is almost isotropic both to the direction of magnetic field and electric current. This isotropy to the direction of magnetic field is clear from the comparison of Figs. 6 or 7, where the magnetic field $\boldsymbol{B}$ is applied parallel to conducting x-y planes, with other figures, e.g., Figs. 3–5 where the magnetic field $\boldsymbol{B}||z$ is normal to conducting layers. This isotropy excludes various orbital magnetoresistance mechanisms common to XMR [6]. Besides the classical magnetoresistance [41,42], there are many other orbital mechanisms of strong interlayer magnetoresistance, pertinent to very anisotropic metals in a field perpendicular to conducting layers [43–49]. These mechanisms, although being present, are not the main source of the observed GMR in κ-(BEDT-TTF)$_2$Hg(SCN)$_2$Br because of (i) its nearly isotropy to the direction of magnetic field and (ii) the strong nonmonotonic pressure dependence with the maximum at Mott MIT.

At first glance, the observed strong influence of a rather weak Zeeman splitting $E_Z \approx eB\hbar/m_e c \lesssim 10$ K at field $B \lesssim 10$ T on a MIT with a much larger energy scale $\gtrsim T_{\rm MI} = 90$ K is very surprising. The bandwidth and e-e interaction competing in this Mott transition have an even larger energy scale. However, even a much smaller field $B \sim 1\,T$ at the field-cooling regime already gives a considerable effect, as shown in Fig. 7. This puzzling behavior is explained by our model where even a small Zeeman splitting strongly affects the spin-glass state by aligning a considerable part of electron spins along the magnetic field, as supported by both the theory of spin-glass behavior [33,34] and the observed strong enhancement of magnetic susceptibility in κ-(BEDT-TTF)$_2$Hg(SCN)$_2$Br at low temperature [12]. It is the Pauli exclusion principle rather than the small Zeeman splitting which prevents electron transport in our GMR mechanism.

In our system, the Mott phase transition spans a remarkably wide pressure interval. Throughout the entire pressure range of our experiment, both metallic and Mott-insulating phases coexist. The insulating fraction is evidenced by the temperature-dependent resistivity with insulating behavior at $T < T_{\rm MI} \approx 90$ K (see Fig. 1). The metallic fraction is revealed via magnetic quantum oscillations (see Fig. 8), with metallic domains exceeding the Larmor radius in size. Usually, an external pressure drives the Mott transition much faster, especially in organic conductors which have a rather small elastic modulus. The extended pressure interval of phase coexistence may arise from glassy behavior coupled with the Mott transition. Notably, a strongly enhanced magnetoresistance is in a narrower pressure interval of $\sim$1 kbar (see Fig. 2).

Quantifying the pressure-dependent volume fractions of metallic and insulating phases would provide valuable insight. The simplest approach employs resistivity measurements combined with effective-medium theory for heterogeneous media [50], which can be easily generalized for quasi-2D layered [51] or completely anisotropic conductors [52]. However, this method requires the knowledge of resistivity in the homogeneous metallic and Mott-insulating phases—values that remain unknown in our case. The Fig. 8 inset shows that the dependence $R(p)$ does not saturate at high pressure, even at $p = 8$ kbar. This means that even at our maximum pressures both metallic and dielectric phases persist, precluding determination of the metallic-phase conductivity. Similarly, even at the lowest (ambient) pressure, the resistivity $R(p)$ does not saturate [16]. Consequently, resistivity measurements alone cannot reliably yield phase fractions as a function of pressure.

Some insight on the portion of metallic phase can be obtained by analyzing the amplitude of magnetic quantum oscillations as a function of pressure. However, the measured Shubnikov–de Haas effect is not very convenient for quantitative estimates, as resistivity depends not only on volume

fractions of the two phases but also on their morphology (shape and mutual orientation) [50–52]. The de Haas–van Alphen oscillation amplitude offers a more suitable probe for volume fraction estimation, particularly when domain sizes much exceed the cyclotron radius of conducting electrons. Nevertheless, the unknown MQO amplitude in the pure metallic phase remains a critical limitation, preventing accurate determination of the metallic-phase fraction.

In another organic conductor κ-(BEDT-TTF)$_2$Cu$_2$(CN)$_3$, the phase fractions of metallic and Mott-insulating phases were estimated using the dielectric response at finite frequency [53]. A similar approach could also prove useful for κ-(BEDT-TTF)$_2$Cu[N(CN)$_2$]Cl and κ-(BEDT-TTF)$_2$Hg(SCN)$_2$Br.

Certainly, the proposed magnetoresistance model does not exclude the standard mechanism [7–10] where the magnetic-field induced shift of Mott metal-insulator transition is governed by thermodynamics and the Clausius-Clapeyron relation. Both effects contribute to the observed magnetoresistance. However, neither the standard numerical calculations [7–10] nor our toy model gives quantitative estimates of the predicted magnetoresistance and its hysteresis to be compared with our measurements. The very slow time relaxation and the temperature/energy scale of the observed hysteresis as compared to the Mott transition suggest that the spin-glass state, known to appear in κ-(BEDT-TTF)$_2$Hg(SCN)$_2$Br at $T \sim 10$ K, is relevant. However, additional experimental methods to distinguish these two magnetoresistance mechanisms would be helpful. We can propose several such experiments for further studies.

First, it is a detailed quantitative study of time relaxation of the observed hysteresis. The spin-glass time relaxation may considerably differ from that of the domain-wall motion. Second, the anisotropy of observed hysteretic magnetoresistance with respect to the direction of magnetic field. According to the standard theory [7–10], this anisotropy is pure thermodynamic and completely determined by the anisotropy of magnetization. On contrary, according to our model the effect is nearly isotropic to the direction of magnetic field.

Besides the pressure, the x-ray irradiation varies the sample quality and provides additional driving parameter affecting the Mott transition, as reported in κ-(BEDT-TTF)$_2$Cu[N(CN)$_2$]Cl [54]. The magnetoresistance studies on the samples of various qualities may also help distinguish two magnetoresistance mechanisms in κ-(BEDT-TTF)$_2$Hg(SCN)$_2$Br. The exchange coupling between the electron spins in κ-(BEDT-TTF)$_2$Hg(SCN)$_2$Br can also be affected by a uniaxial strain [55], providing another driving parameter. The uniaxial strain was previously used to shift the MIT in κ-(BEDT-TTF)$_2$Cu$_2$(CN)$_3$ [56].

The proposed GMR mechanism is rather general and may apply to other compounds with Mott metal insulator transition, particularly with spin frustrations. For example, similar GMR effects have been observed in another organic metal, κ-(BEDT-TTF)$_2$Cu[N(CN)$_2$]Cl [11,57,58], and the standard theory [8–10], which neglects the glassy state, may be insufficient to explain all GMR features in this compound. A somewhat similar but more complex pressure-temperature phase diagram appears in κ-(BEDT-TTF)$_2$Cu$_2$(CN)$_3$ [53,56] and EtMe$_3P$[Pd(dmit)$_2$]$_2$ [59], where the Mott MIT also couples with spin frustrations on a triangular lattice. However, in these two organic conductors a negative magnetoresistance is observed in some parametric range [56,59], which probably indicates a competition of two opposite effects of magnetic field on electron transport. Possibly, thermodynamically, the magnetic field favors the metallic rather than insulating phase in these compounds, which leads to negative magnetoresistance, while the other effects of magnetic field increase resistivity. Note that the low-temperature Mott-insulating phase in these two compounds is suggested to have an additional charge ordering, called valence bond solid [56,59]. How this charge ordering affects magnetoresistance remains an open problem beyond the scope of our paper. In κ-(BEDT-TTF)$_2$Hg(SCN)$_2$Br and κ-(BEDT-TTF)$_2$Cu[N(CN)$_2$]Cl, at low temperatures one instead observes a glassy dynamics [12,27], which couples spin and charge degrees of freedom.

V. CONCLUSION

We observe and investigate the giant hysteretic magnetoresistance which accompanies the Mott metal-insulator transition in the organic metal κ-(BEDT-TTF)$_2$Hg(SCN)$_2$Br. The magnetoresistance and hysteresis are the strongest at low temperature and the pressure around 3 kbar, corresponding to the Mott-Habbard phase transition. At our lowest temperature $T = 0.5$ K, the hysteresis width reaches the interval $\Delta B \approx 4$ T and the ratio $R(B)/R(0) \approx 30$ in a field $B \approx 16.5$ T. Notably, this hysteretic magnetoresistance is almost isotropic with respect to the direction of magnetic field. In particular, it is observed also for the field parallel to the conducting layers, which excludes the orbital effect of magnetic field as an origin of this phenomenon and points to its coupling to electron spin. In the organic metal κ-(BEDT-TTF)$_2$Hg(SCN)$_2$Br, the behavior of the spin system is complicated by antiferromagnetic frustrations on the triangular lattice, which differs our system from the standard theory [8–10] of Mott transition in a magnetic field. The observed temperature dependence of hysteresis, together with the relaxation time values and their dependence on magnetic field (see Fig. 7), confirm the influence of spin-glass on magnetoresistance. We propose an explanation and a toy model giving qualitatively this unusual magnetoresistance behavior, which differ from the known giant magnetoresistance mechanisms. We suggest the observed effect as another class of extreme magnetoresistance phenomena, which couples the physics of strongly correlated electrons and GMR.

ACKNOWLEDGMENTS

The work was partially supported by the state assignment of the FRC PCP MC RAS (Registration No. 124013100858-3) and the state assignment of ISSP RAS. P.D.G. acknowledges state assignment No. FFWR-2024-0015.

DATA AVAILABILITY

The data that support the findings of this article are not publicly available upon publication because it is not technically feasible and/or the cost of preparing, depositing, and hosting the data would be prohibitive within the terms of this research project. The data are available from the authors upon reasonable request.

[1] P. A. Grünberg, Nobel lecture: From spin waves to giant magnetoresistance and beyond, Rev. Mod. Phys. **80**, 1531 (2008).

[2] I. Ennen, D. Kappe, T. Rempel, C. Glenske, and A. Hütten, Giant magnetoresistance: Basic concepts, microstructure, magnetic interactions and applications, Sensors **16**, 904 (2016).

[3] A. P. Ramirez, Colossal magnetoresistance, J. Phys.: Condens. Matter **9**, 8171 (1997).

[4] E. Tafra, N. Novosel, Z. Skoko, T. Ivek, M. Basletić, B. Mihaljević, Z. Jagličić, D. R. Góngora, S. Tomić, A. Hamzić, V. Roddatis, F. Fischgrabe, V. Moshnyaga, B. Korin-Hamzić, and M. Čulo, Colossal magnetoresistance effect and spin-dependent variable-range hopping in the charge ordered phase of overdoped (La, Ca)MnO_3 manganites, Phys. Rev. B **111**, 115107 (2025).

[5] S. Balguri, M. B. Mahendru, Enrique O. G. Delgado, K. Fruhling, X. Yao, D. E. Graf, J. A. Rodriguez-Rivera, A. A. Aczel, T. J. Hicken, H. Luetkens, M. J. Graf, A. Rydh, J. Gaudet, and F. Tafti, Two types of colossal magnetoresistance with distinct mechanisms in $Eu_5In_2As_6$, Phys. Rev. B **111**, 115114 (2025).

[6] R. Niu and W. K. Zhu, Materials and possible mechanisms of extremely large magnetoresistance: A review, J. Phys.: Condens. Matter **34**, 113001 (2022).

[7] W. F. Brinkman and T. M. Rice, Application of Gutzwiller's variational method to the metal-insulator transition, Phys. Rev. B **2**, 4302 (1970).

[8] L. Laloux, A. Georges, and W. Krauth, Effect of a magnetic field on Mott-Hubbard systems, Phys. Rev. B **50**, 3092 (1994).

[9] M. J. Rozenberg, G. Kotliar, and X. Y. Zhang, Mott-Hubbard transition in infinite dimensions. II, Phys. Rev. B **49**, 10181 (1994).

[10] A. Georges, G. Kotliar, W. Krauth, and M. J. Rozenberg, Dynamical mean-field theory of strongly correlated fermion systems and the limit of infinite dimensions, Rev. Mod. Phys. **68**, 13 (1996).

[11] F. Kagawa, T. Itou, K. Miyagawa, and K. Kanoda, Magnetic-field-induced Mott transition in a quasi-two-dimensional organic conductor, Phys. Rev. Lett. **93**, 127001 (2004).

[12] M. Hemmida, H.-A. Krug von Nidda, B. Miksch, L. L. Samoilenko, A. Pustogow, S. Widmann, A. Henderson, T. Siegrist, J. A. Schlueter, A. Loidl, and M. Dressel, Weak ferromagnetism and glassy state in κ-(BEDT-TTF)$_2$Hg(SCN)$_2$Br, Phys. Rev. B **98**, 241202(R) (2018).

[13] N. Hassan, S. Cunningham, M. Mourigal, E. I. Zhilyaeva, S. A. Torunova, R. N. Lyubovskaya, J. A. Schlueter, and N. Drichko, Evidence for a quantum dipole liquid state in an organic quasi–two-dimensional material, Science **360**, 1101 (2018).

[14] T. Ishiguro, K. Yamaji, and G. Saito, *Organic Superconductors* (Springer, Berlin, 1998)

[15] T. Mori, H. Mori, and S. Tanaka, Structural genealogy of BEDT-TTF-based organic conductors II. Inclined molecules: θ, α and κ phases, Bull. Chem. Soc. Jpn. **72**, 179 (1999).

[16] S. I. Pesotskii, R. B. Lyubovskii, G. V. Shilov, V. N. Zverev, S. A. Torunova, E. I. Zhilyaeva, and E. Canadell, Effect of external pressure on the metal–insulator transition of the organic quasi-two-dimensional metal κ-(BEDT-TTF)$_2$Hg(SCN)$_2$Br, Magnetochemistry **8**, 152 (2022).

[17] T. Ivek, R. Beyer, S. Badalov, M. Čulo, S. Tomić, J. A. Schlueter, E. I. Zhilyaeva, R. N. Lyubovskaya, and M. Dressel, Metal-insulator transition in the dimerized organic conductor κ-(BEDT-TTF)$_2$Hg(SCN)$_2$Br, Phys. Rev. B **96**, 085116 (2017).

[18] N. M. Hassan, K. Thirunavukkuarasu, Z. Lu, D. Smirnov, E. I. Zhilyaeva, S. Torunova, R. N. Lyubovskaya, and N. Drichko, Melting of charge order in the low-temperature state of an electronic ferroelectric-like system, npj Quantum Mater. **5**, 15 (2020).

[19] T. Le, A. Pustogow, J. Wang, A. Henderson, T. Siegrist, J. A. Schlueter, and S. E. Brown, Disorder and slowing magnetic dynamics in κ-(BEDT-TTF)$_2$Hg(SCN)$_2$Br, Phys. Rev. B **102**, 184417 (2020).

[20] See Supplemental Material at http://link.aps.org/supplemental/10.1103/j565-gnd6 for the calculation of conductivity of antiferromagnet-driven resistor lattices.

[21] This estimate has a simple physical meaning: Due to lowering of the energy of filled electron states by the formation of energy gap, each electron at the Fermi level gains the energy $\sim E_g/2$. The fraction of such electrons at the Fermi level is $\nu \sim E_g/E_F$. Hence, the total energy gain per electron is $\sim \nu E_g \sim E_g/E_F$.

[22] K. Aryanpour, W. E. Pickett, and R. T. Scalettar, Dynamical mean-field study of the Mott transition in the half-filled Hubbard model on a triangular lattice, Phys. Rev. B **74**, 085117 (2006).

[23] T. Shirakawa, T. Tohyama, J. Kokalj, S. Sota, and S. Yunoki, Ground-state phase diagram of the triangular lattice Hubbard model by the density-matrix renormalization group method, Phys. Rev. B **96**, 205130 (2017).

[24] A. Vranić, J. Vučičević, J. Kokalj, J. Skolimowski, R. Žitko, J. Mravlje, and D. Tanasković, Charge transport in the Hubbard model at high temperatures: Triangular versus square lattice, Phys. Rev. B **102**, 115142 (2020).

[25] A. Wietek, R. Rossi, F. Šimkovic, M. Klett, P. Hansmann, M. Ferrero, E. M. Stoudenmire, T. Schäfer, and A. Georges, Mott insulating states with competing orders in the triangular lattice Hubbard model, Phys. Rev. X **11**, 041013 (2021).

[26] K. J. Kapcia, Charge-order on the triangular lattice: A mean-field study for the lattice $s = 1/2$ fermionic gas, Nanomaterials **11**, 1181 (2021).

[27] J. Müller and T. Thomas, Low-frequency dynamics of strongly correlated electrons in (BEDT-TTF)$_2$X studied by fluctuation spectroscopy, Crystals **8**(4), 166 (2018).

[28] G. Kotliar, S. Y. Savrasov, K. Haule, V. S. Oudovenko, O. Parcollet, and C. A. Marianetti, Electronic structure calculations with dynamical mean-field theory, Rev. Mod. Phys. **78**, 865 (2006).

[29] Y. S. Lyakhova, G. V. Astretsov, and A. N. Rubtsov, Mean-field concept and post-DMFT methods in the modern theory of correlated systems, Phys. Usp. **66**, 775 (2023).

[30] Y. Saito and K. Igeta, Antiferromagnetic Ising model on a triangular lattice, J. Phys. Soc. Jpn. **53**, 3060 (1984).

[31] F. Barrows, E. Iacocca, and F. Caravelli, Resistive Ising: Effective resistance in random magnetic nanowire networks, Phys. Rev. E **112**, 014302 (2025).

[32] V. J. Dowling and Y. V. Pershin, Memristive Ising circuits, Phys. Rev. E **106**, 054156 (2022).

[33] V. S. Dotsenko, Physics of the spin-glass state, Phys. Usp. **36**, 455 (1993).

[34] V. Dotsenko, *An Introduction to the Theory of Spin Glasses and Neural Networks* (World Scientific, Singapore, 1995).

[35] P. C. W. Leung, T. J. Emge, M. A. Beno, H. H. Wang, J. M. Williams, V. Petricek, and P. Coppens, Novel structural modulation in the ambient-pressure sulfur-based organic superconductor.beta.-(BEDT-TTF)2I3: origin and effects on its electrical conductivity, J. Am. Chem. Soc. **107**, 6184 (1985).

[36] A. J. Schultz, H. H. Wang, J. M. Williams, and A. Filhol, Effect of structural disorder on organic superconductors: A neutron diffraction body of "high-Tc".beta.*-(bis(ethylenedithio)tetrathiafulvalene)2 triiodide at 4.5 K and 1.5 kbar, J. Am. Chem. Soc. **108**, 7853 (1986).

[37] B. Hartmann, J. Müller, and T. Sasaki, Mott metal-insulator transition induced by utilizing a glasslike structural ordering in low-dimensional molecular conductors, Phys. Rev. B **90**, 195150 (2014).

[38] D. Guterding, R. Valentí, and H. O. Jeschke, Influence of molecular conformations on the electronic structure of organic charge transfer salts, Phys. Rev. B **92**, 081109(R) (2015).

[39] J. Liebman, K. Miyagawa, K. Kanoda, and N. Drichko, Novel dipole-lattice coupling in the quantum spin liquid material κ-(BEDT-TTF)$_2$Cu$_2$(CN)$_3$, Phys. Rev. B **110**, 165105 (2024).

[40] P. A. Lee and T. V. Ramakrishnan, Disordered electronic systems, Rev. Mod. Phys. **57**, 287 (1985).

[41] A. A. Abrikosov, *Fundamentals of the Theory of Metals* (Elsevier Science Pub. Co, Amsterdam, 1988).

[42] J. M. Ziman, *Principles of the Theory of Solids* (Cambridge University Press, Cambridge, England, 1972).

[43] V. M. Gvozdikov, Incoherence, metal-to-insulator transition, and magnetic quantum oscillations of interlayer resistance in an organic conductor, Phys. Rev. B **76**, 235125 (2007).

[44] M. V. Kartsovnik, P. D. Grigoriev, W. Biberacher, and N. D. Kushch, Magnetic field induced coherence-incoherence crossover in the interlayer conductivity of a layered organic metal, Phys. Rev. B **79**, 165120 (2009).

[45] P. D. Grigoriev, Weakly incoherent regime of interlayer conductivity in a magnetic field, Phys. Rev. B **83**, 245129 (2011).

[46] P. D. Grigoriev, Monotonic growth of interlayer magnetoresistance in strong magnetic field in very anisotropic layered metals, JETP Lett. **94**, 47 (2011).

[47] P. D. Grigoriev, M. V. Kartsovnik, and W. Biberacher, Magnetic-field-induced dimensional crossover in the organic metal α-(BEDT-TTF)$_2$KHg(SCN)$_4$, Phys. Rev. B **86**, 165125 (2012).

[48] P. D. Grigoriev, Longitudinal interlayer magnetoresistance in strongly anisotropic quasi-two-dimensional metals, Phys. Rev. B **88**, 054415 (2013).

[49] A. A. Sinchenko, P. D. Grigoriev, P. Lejay, and P. Monceau, Linear magnetoresistance in the charge density wave state of quasi-two-dimensional rare-earth tritellurides, Phys. Rev. B **96**, 245129 (2017).

[50] S. Torquato, *Random Heterogeneous Materials* (Springer, New York, 2002).

[51] A. A. Sinchenko, P. D. Grigoriev, A. P. Orlov, A. V. Frolov, A. Shakin, D. A. Chareev, O. S. Volkova, and A. N. Vasiliev, Gossamer high-temperature bulk superconductivity in FeSe, Phys. Rev. B **95**, 165120 (2017).

[52] S. S. Seidov, K. K. Kesharpu, P. I. Karpov, and P. D. Grigoriev, Conductivity of anisotropic inhomogeneous superconductors above the critical temperature, Phys. Rev. B **98**, 014515 (2018).

[53] R. Rösslhuber, A. Pustogow, E. Uykur, A. Böhme, A. Löhle, R. Hübner, J. A. Schlueter, Y. Tan, V. Dobrosavljević, and M. Dressel, Phase coexistence at the first-order Mott transition revealed by pressure-dependent dielectric spectroscopy of κ − (BEDT-TTF)$_2$-Cu$_2$(CN)$_3$, Phys. Rev. B **103**, 125111 (2021).

[54] E. Gati, U. Tutsch, A. Naji, M. Garst, S. Köhler, H. Schubert, T. Sasaki, and M. Lang, Effects of disorder on the pressure-induced Mott transition in κ-(BEDT-TTF)$_2$Cu[N(CN)$_2$]Cl, Crystals **8**(1), 38 (2018).

[55] J. Liebman, S. Torunova, J. A. Schlueter, E. Zhilyaeva, and N. Drichko, Tuning charge order in κ-(BEDT-TTF)$_2$Hg(SCN)$_2$X (X=Br, Cl) via uniaxial strain, arXiv:2503.11547.

[56] Y. Kawasugi, S. Yamazaki, A. Pustogow, and N. Tajima, Negative magnetoresistance near the mott metal–insulator transition in the quantum spin liquid candidate κ-(BEDT-TTF)$_2$Cu$_2$(CN)$_3$, J. Phys. Soc. Jpn. **92**, 065001 (2023).

[57] S. Oberbauer, S. Erkenov, W. Biberacher, N. D. Kushch, R. Gross, and M. V. Kartsovnik, Coherent heavy charge carriers in an organic conductor near the bandwidth-controlled Mott transition, Phys. Rev. B **107**, 075139 (2023).

[58] S. Erkenov, S. Fust, S. Oberbauer, W. Biberacher, N. D. Kushch, H. Müller, F. L. Pratt, R. Gross, and M. V. Kartsovnik, Electronic correlations and spin frustration in the molecular conductors κ-(BEDT-TTF)$_2X$ probed by magnetic quantum oscillations, Phys. Rev. B **110**, 205149 (2024).

[59] Y. Shimizu, H. Akimoto, H. Tsujii, A. Tajima, and R. Kato, Mott transition in a valence-bond solid insulator with a triangular lattice, Phys. Rev. Lett. **99**, 256403 (2007).